Patterning flood illumination with microlens arrays

Ming-Hsien Wu, Kateri E. Paul, and George M. Whitesides

We describe a convenient lithographic technique that can produce simple, repetitive micropatterns over large areas (several square centimeters). The technique uses an illuminated array of micrometer-scale lenses to generate an array of optical patterns in an image plane located within micrometer distances from the lens array. A layer of photoresist, placed in the image plane, records the patterns. Microlenses with different sizes, profiles, composition, and indices of refraction produce corresponding patterns in exposed and developed photoresist. Both spherical and nonspherical microlenses were examined. Several types of optical element containing arrays of microlenses were fabricated and used to demonstrate that this technique can generate uniform micropatterns over large areas (>4 cm^2) in a single exposure. The smallest features produced had dimensions of $\sim$100 nm. © 2002 Optical Society of America

OCIS codes: 350.3950, 110.5220, 220.3630, 350.3850, 160.5470, 110.3960.

1. Introduction

A. Background

Arrays of micropatterns are useful for a wide range of applications; examples include optical filters,[1–3] photonic crystals,[4] digital optical systems,[5,6] and displays.[7,8] Conventional photolithography,[9] holographic lithography,[10] *e*-beam lithography,[11] and laser pattern writing[12] are currently used to fabricate repetitive micropatterns. Although these techniques produce high-quality patterns, they require expensive facilities and involve multistep processing. In this paper we demonstrate a process for large-area fabrication of repetitive arrays of micropatterns that does not require those techniques. We begin this method by fabricating an array of microlenses supported on a thin, transparent, elastomeric membrane whose thickness is the focal length of the lens. This array of microlenses patterns incident illumination and produces an optical pattern that depends on the pattern of the lens array. We place a layer of photoresist on the plane of the optical pattern to record it; the exposed and developed photoresist shows the distribution of light from the optical pattern. We use both spherical and nonspherical microlenses. These two types of microlense generate a different type of pattern: A two-dimensional (2-D) crystal of transparent microspheres produces a dense, hexagonal array of micropatterns[8,13,14]; a microlens array fabricated by photolithography or soft lithography generates an array of micropatterns whose form depends on the structures of the microlens array.[15,16] This simple technique can produce repetitive arrays of micropatterns with feature sizes as small as 100 nm, in parallel, over an area >4 cm^2.

We first describe use of arrays of crystalline (hexagonal close packed), transparent microspheres embedded in a transparent elastomeric matrix to produce micropatterns in photoresist. We then discuss the fabrication and use of microlens arrays for the generation of arrays of micropatterns in nonhexagonal arrangements.

B. Transparent Microspheres

Transparent microspheres act as ball lenses and exhibit a range of optical phenomena including lensing[8,13,14,17] (Fig. 1) and light scattering.[18–21] A range of applications based on these phenomena has been proposed.[14,22–24] Individual microspheres can be used as microobjectives[22,23] or rotational probes for microscopy,[24] and crystallization of microspheres forms periodic dielectric microstructures that can function as photonic crystals[25,26] and arrays of projection microlenses.[14]

Transparent microspheres can cause illumination to converge or diverge, depending on the ratio of re-

The authors are with the Department of Chemistry and Chemical Biology, 12 Oxford Street, Harvard University, Cambridge, Massachusetts 02138. The e-mail address for G. M. Whitesides is gwhitesides@gmwgroup.harvard.edu.

n_s: refractive index of microlenses
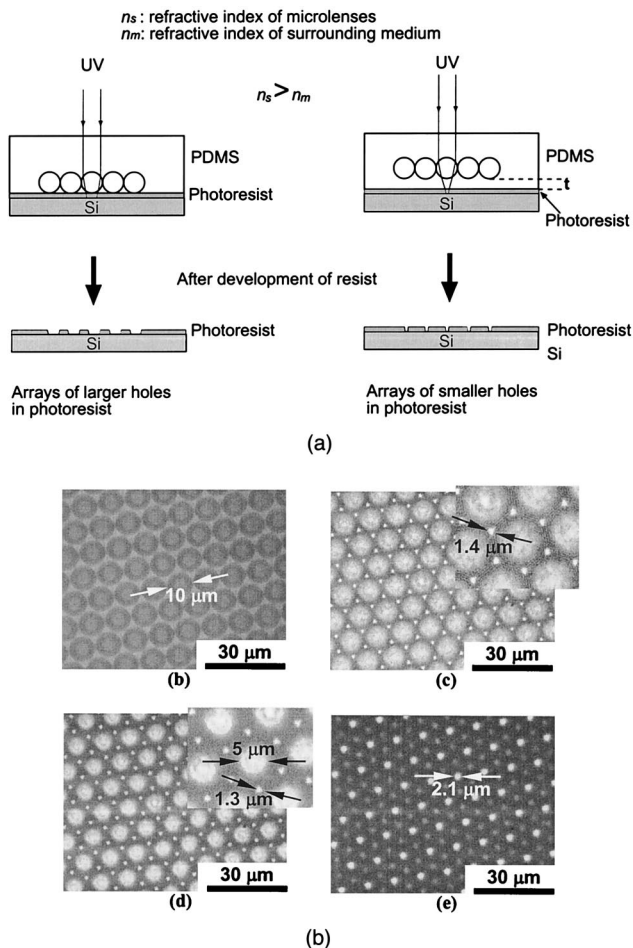n_m: refractive index of surrounding medium

$n_s > n_m$

(a)

(b)

Fig. 1. (a) Schematic illustration comparing patterns formed by use of PDMS membranes with (left) and without (right) a spacer of thickness t between the embedded spheres and the surfaces of the membranes. Note that use of the spacer shown on the right-hand side localizes the light in the photoresist layer more than without the spacer and results in smaller patterns. (b) Photomicrograph of a 2-D crystal of 10-μm polystyrene spheres. (c)–(e) A series of optical micropatterns produced by the 10-μm polystyrene spheres with image distance $d_i = -0.8, 0.0,$ and 4.6 μm, respectively. The orientation of the array of microspheres is the same in each picture.

microlenses, and this array produces a correspondingly dense optical pattern. We use 2-D crystals of microspheres for photolithography to generate patterns in a layer of photoresist.

Because the optical patterns in photoresist produced by an array of microlenses depend on the distance d_P between the array and the photoresist, we can obtain a series of different micropatterns in photoresist by tuning d_P.[16] Figure 1(a) shows that an array of microlenses generates an array of spots smaller than the microlenses when a spacer with thickness smaller than the focal length is placed between the microlenses and the layer of resist. Figure 1(b) shows a top view of a 2-D crystal of 10-μm spheres. Figures 1(c)–(e) show three optical patterns produced by the 2-D crystal of 10-μm spheres on a series of image planes with increasing image distance d_i. These optical patterns were generated at $d_i = -0.8, 0.0,$ and 4.6 μm, respectively. The patterns shown in Figs. 1(c) and 1(d) were produced by interference of the light from neighboring spheres. Figure 1(e) shows an array of bright spots produced on the focal plane of the 2-D array of microspheres.

To facilitate a uniform spacing between the microlens array and the layer of resist, we used two types of spacer: (i) an elastomeric thin film [polydimethylsiloxane (PDMS), $n_{\mathrm{PDMS}} = 1.4$, Sylgard 184, Dow Corning] with a uniform thickness and (ii) a uniform air gap ($n_{\mathrm{air}} = 1$) between the microlenses and the photoresist. We used elastomeric thin films in near-field, contact-mode photolithography to provide a conformal contact between optical elements and a layer of resist.[27–30] Although the deformation of patterned PDMS membranes causes distortion of patterns in soft lithography,[27] deformation is relatively unimportant when we use the flat sheet of PDMS that serves as the optical element in this research. Patterns generated by this technique depend on the lensing of rigid microlenses, rather than on the optics of a deformable, patterned PDMS membrane, and the membrane serves primarily to ensure uniform spacing of the lenses from the photoresist layer and to eliminate an air gap in the optical path from the lens to the photoresist.

Because the refractive index of the elastomeric thin films ($n_m = n_{\mathrm{PDMS}} = 1.4$) is higher than that of an air gap ($n_m = n_{\mathrm{air}} = 1$), the thin film lowers the contrast of refractive indices between the lenses and the surrounding medium (n_l:n_m). The lowered contrast of refractive indices reduces the concentration of light passing through the lens array and also reduces the resolution of the optical patterns. We can improve the resolution by incorporating a uniform air gap between the lens array and the photoresist, although it is technically difficult to maintain a uniform micrometer-size gap over a large area.

C. Fabricated Microlens Arrays

We also used arrays of plano–convex microlenses. We fabricated arrays of these microlenses using three techniques: (i) melting and reflow of photoresist[15,31,32]; (ii) self-assembly of liquid polymers on
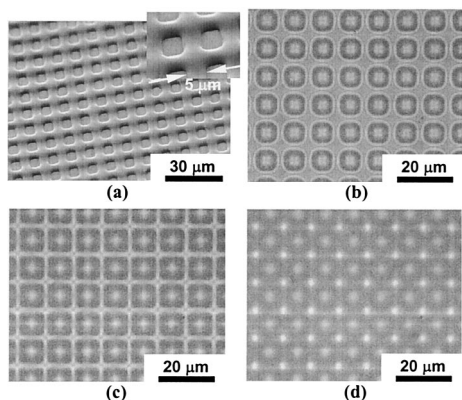
fractive indices between the spheres (n_s) and the surrounding medium (n_m). Although this lensing can be rigorously described with Mie theory,[20,21] the formulas that emerge from the theory are inconvenient to use. Here we use simple arguments from geometric optics to explain lensing by spherical microlenses under two conditions. (i) Individual spheres illuminated by collimated light: A low-index sphere ($n_s < n_m$) causes incident illumination to diverge, whereas a high-index sphere ($n_s > n_m$) causes incident illumination to converge and produces a bright spot on its focal plane. (ii) 2-D hexagonal close-packed crystals of spheres under collimated illumination: Each sphere receives light scattered from its six neighboring spheres and the array of microspheres produces a hexagonal array of optical patterns with six sides. A 2-D crystal of microspheres forms a compact array of

Fig. 2. (a) SEM image of a 5 μm × 5 μm grid lens. (b)–(d) Photomicrographs of a series of optical micropatterns generated by the grid lens shown in (a) with image distance d_i = 5, 8.3, and 19 μm, respectively.

patterned, functionalized surfaces[16,33–35]; and (iii) molding, using techniques such as replica molding[36] and solvent-assisted embossing.[37] We used methods (i) and (ii) to fabricate microlens arrays on glass substrates and used method (iii) to fabricate microlens arrays on elastomeric membranes.

A patterned microlens array also generates a pattern of images; these images will be different on different image planes. Figure 2(a) shows a scanning electron microscope (SEM) image of a 5 μm × 5 μm grid lens. Figures 2(b)–2(d) show the optical patterns produced by the grid lens on different image planes with image distance d_i = 5.0, 8.3, and 19 μm, respectively. The grid lens shown in Fig. 2 generated optical patterns in a square pattern, but this pattern is fixed by the pattern of the grid and can be changed by design. These optical patterns are uniform over an area larger than 4 cm². The optical patterns in some image planes contain submicrometer features.

2. Experimental Procedure

A. Preparation of Optical Elements Containing Microlens Arrays

We prepared four types of an optical element based on microlenses. Each type uses microlenses that direct incident illumination in a particular way: (i) high-index microlenses that cause light to converge, (ii) low-index microlenses that cause light to diverge, (iii) lenses spaced from the photoresist by a spacer or a gap, and (iv) lenses in an array situated at an oblique angle to the incident illumination.

1. Polydimethylsiloxane Membrane with an Embedded Monolayer of Microspheres

Figure 1(a) compares lensing by spheres embedded at different depths inside a membrane. On the left-hand side a PDMS spacer with a thickness t separates the embedded spheres from the surface of the membrane. Incident illumination is concentrated by each sphere and further propagates through the
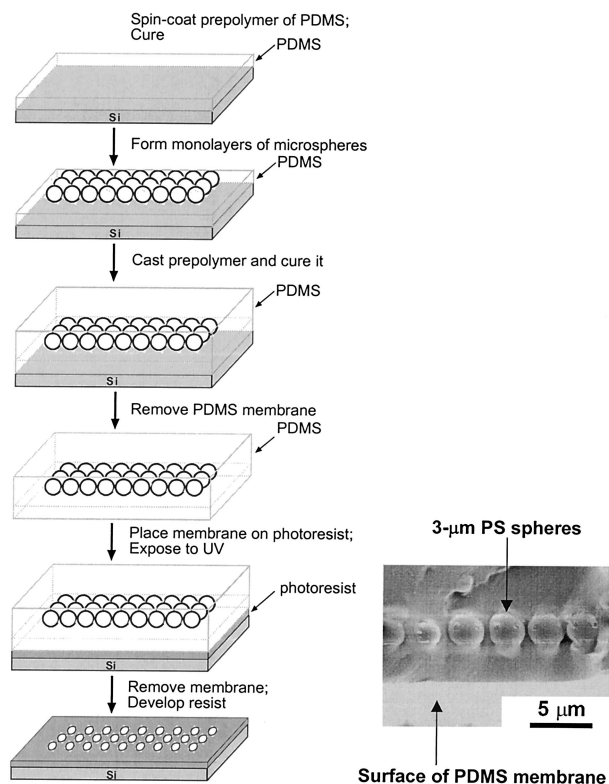

Fig. 3. Illustration of the fabrication of a PDMS membrane with a 2-D crystalline array of embedded microspheres. The spheres are separated from the surface of the membrane by a distance t, equal to the thickness of the PDMS spacer.

spacer to form patterns of illumination. Spacers with different thickness generate different patterns.

Figure 3 summarizes the procedure used to generate PDMS membranes containing embedded microspheres. The membranes were prepared on silicon wafers passivated with a thin film of polyfluorosilane (tridecafluoro-1,1,2,2-tetrahydrooctyltrichlorosilane, United Chemical Technologies, Inc., Bristol, Pa.). We spin coated (spin speed of 1500 rpm) the passivated silicon wafer with a thin film of a PDMS prepolymer diluted in heptane (PDMS prepolymer: heptane of 1:5.5 for a 3-μm-thick layer of PDMS). This solution yielded a PDMS film with a uniform thickness of $t \cong$ 1–20 μm after curing. The silanization prevented adhesion of the PDMS to the wafer. To crystallize microspheres on the PDMS thin film, we first oxidized its exposed surface in an oxygen plasma in a laboratory plasma cleaner for 15 s to make it hydrophilic. We then placed a dilute aqueous suspension of microspheres on the oxidized surface.[38] Slow evaporation of the water generated a polycrystalline monolayer of microspheres. We exposed the PDMS thin film and the arrays of crystallized spheres to an oxidizing plasma for 15 s to produce a layer of oxidized PDMS that adheres well to a second, thicker film (~3 mm) of PDMS cast over the thin film. This composite formed a flexible membrane. The second layer of PDMS completely fills the gaps between the spheres and the first layer of

the PDMS. We made the top surface of the membrane flat by using gravity for leveling. To facilitate removal of the cured membrane from the surface of the wafer, and to minimize tearing of the membrane, the membrane was peeled away from the substrate with the system immersed in ethanol. The combination of silanization of the silicon surface, and oxidization of the first layer of PDMS and arrays of microspheres to form a seal with the second layer of PDMS, prevented the microspheres from sticking to the substrate; all the microspheres remained embedded in the membrane.

2. Polydimethylsiloxane Membrane with a Monolayer of Air Microspheres in the Surface

Air spheres have the lowest achievable refractive index (n_{air} = 1). This type of membrane uses what are, in essence, air lenses to cause incident light to diverge and to produce protrusive micropatterns in positive photoresist. We prepared a PDMS membrane by the procedure described above in such a way that it had a monolayer of polystyrene (PS) microspheres embedded in its surface. On sonication of this membrane in acetone, the PS spheres dissolved. After the removal of the spheres, we cleaned and dried the membrane under a stream of nitrogen. This procedure generated a membrane with a monolayer of approximately spherical holes in the surface.

3. Wedge-Shaped Polydimethylsiloxane Membrane with a Monolayer of Microspheres Embedded in the Surface

Wedge-shaped membranes refract incident illumination to an angle $\alpha = \sin^{-1}(\sin\theta/n_{PDMS})$, and the embedded spheres receive incident light at an angle $\beta = \theta - \sin^{-1}(\sin\theta/n_{PDMS})$ according to Snell's law (Fig. 4). This deflection of light results in a change in the pattern formed in the photoresist. To obtain wedge-shaped membranes containing embedded microspheres, we prepared a monolayer of crystallized spheres on a thin uniform membrane by the same procedure described above. We tilted the sphere-covered substrate at an angle θ and cast a second layer of PDMS on it. After removal of the PDMS from the substrate, we obtained a wedge-shaped PDMS membrane with microspheres embedded in the surface. Figure 4 illustrates fabrication for this type of membrane.

4. Transparent Membrane with an Array of Plano–Convex Microlenses Embedded Inside the Membrane

We used three methods to fabricate arrays of microlenses on glass substrates: (i) melting and reflow of photoresist [Fig. 5(a)], (ii) self-assembly of liquid polymers on functionalized surfaces [Fig. 5(b)], and (iii) solvent-assisted embossing [Fig. 5(c)]. We also used replica molding to fabricate microlens arrays on elastomeric membranes.

For uniform lensing, the medium between a microlens array and the photoresist should be a thin transparent film with a uniform thickness. We used

$$\beta = \theta - \sin^{-1}(\sin(1/n_{PDMS}))$$
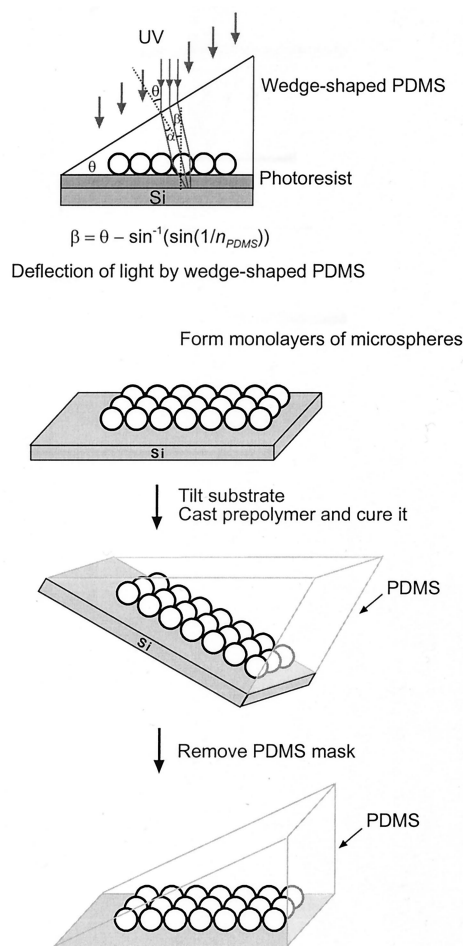
Deflection of light by wedge-shaped PDMS

Fig. 4. Fabrication of wedge-shaped membranes with a 2-D array of microspheres embedded in the surface. The top figure illustrates the oblique illumination on microspheres with a wedge-shaped membrane.

two types of media: (i) PDMS as a thin film and (ii) an air gap. For (i), we spin coated a microlens array with a PDMS thin film; this thin film served as a spacer with a thickness equal to the image distance. For (ii), we fabricated PDMS spacers on the edges of the lens array. The thickness of these spacers was chosen to be equal to the image distance when the lens array was operating in air. The layer of photoresist to be patterned was placed on top of the spacers; this configuration produced a uniform air gap between the resist layer and the lens array [Fig. 5(a)]. Generally, it is easier to use PDMS spacers rather than air gaps for uniform microlensing over large areas, although the higher index (n_{PDMS} = 1.4) of PDMS spacers can lower the convergence of the illumination on the photoresist.

We fabricated an array of microlenses on two types of transparent substrates: a rigid substrate of glass and an elastomeric membrane of PDMS. An array of microlenses fabricated on a rigid substrate generates an array of micropatterns with the patterns having the same arrangement as in the plane of the microlenses. This method has the advantage that
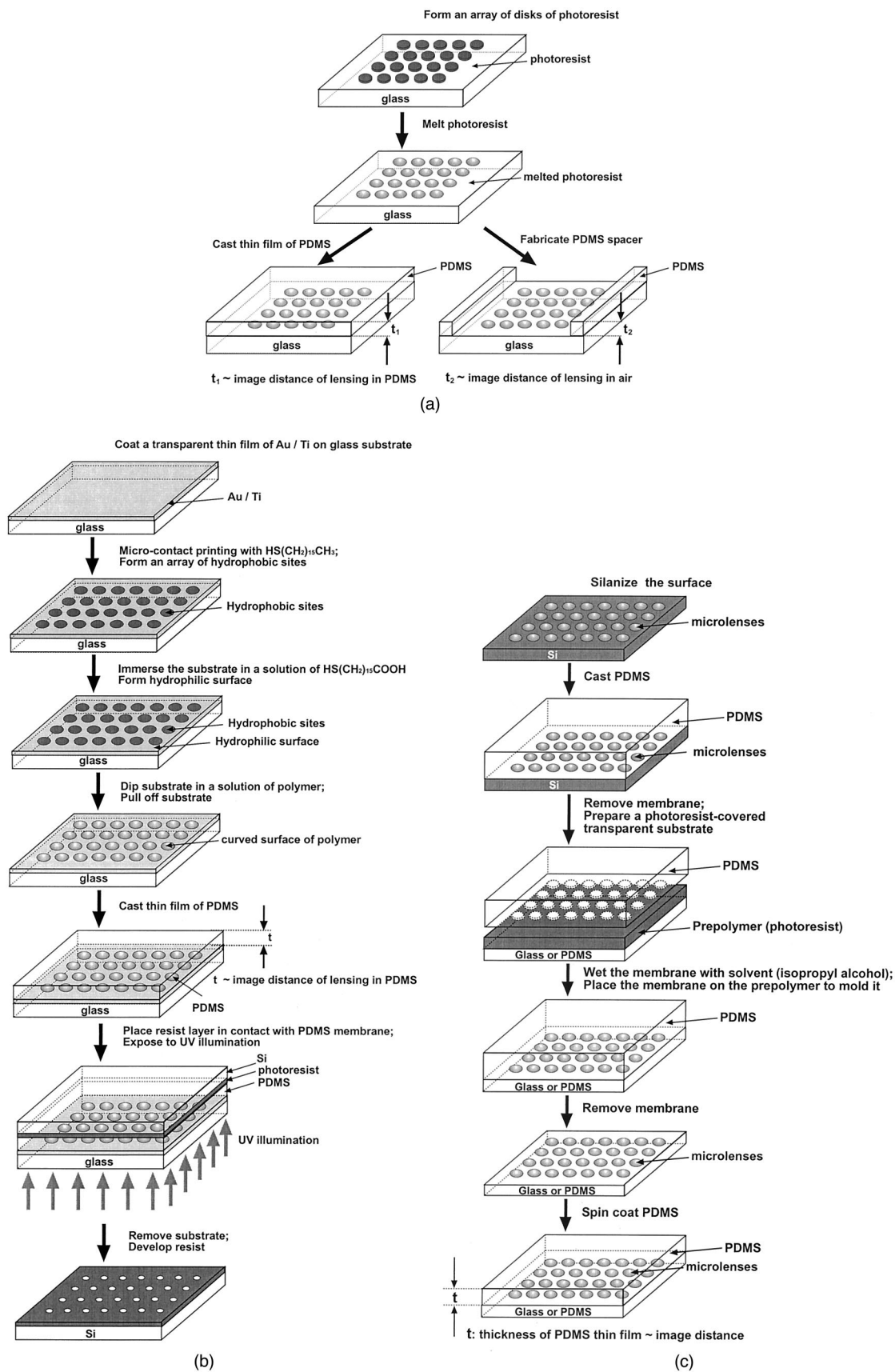
Fig. 5. Fabrication of microlenses by various methods: (a) melting and reflow of photoresist, (b) self-assembly of liquid polymers on functionalized surfaces, (c) solvent-assisted embossing.
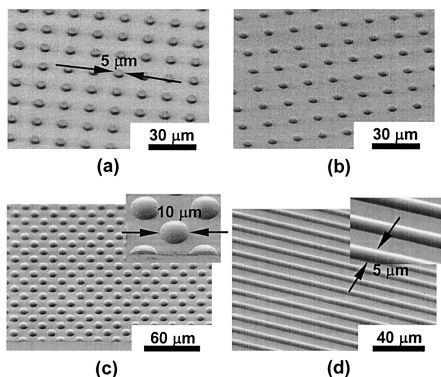
Fig. 6. SEM images of plano–convex microlenses with different shapes and arrangements. (a) A square array of 5-μm circular disks of photoresist with a 15-μm pitch; (b) the disks of photoresist were melted on a hot plate, and the reflow of photoresist formed a curved surface; (c) a square array of 10-μm plano–convex lenses; (d) A 5 μm × 5 μm array of cylindrical microlenses.

Fig. 7. Absorption spectrum of PDMS. This spectrum shows that PDMS (as a membrane ∼1 cm thick) absorbs less than 5% of incident UV illumination for the wavelength ranging from 365 to 436 nm. PDMS is transparent to UV light in this wavelength range.

there is little variation in the lateral position of the patterns. Elastomeric membranes offer the advantage that they can pattern uneven or curved surfaces to which rigid membranes cannot be applied, but have the disadvantage that there is some variation in the period in the in-plane registration of the micropatterns that is due to the elasticity of the membrane.[39]

Figure 6 shows SEM pictures of representative microlenses fabricated by the reflow method described above. Figure 6(a) shows an array of 5-μm circular disks of photoresist with a period of 15 μm. The disks of photoresist were melted on a hot plate, and the reflow of photoresist formed the curved surfaces shown in Fig. 6(b). An array of plano–convex microlenses formed on cooling the substrate. Figures 6(c) and 6(d) show representative microlens arrays: a square array of 10-μm plano–convex lenses and a 5 μm × 5 μm array of cylindrical lenses, respectively.

B. Photolithography

To carry out contact-mode photolithography, we placed a PDMS membrane containing embedded microspheres or microlenses on a substrate spin coated with 0.4–1.4-μm-thick positive-tone photoresist (1800 series, Shipley, n_{PR} = 1.7); the membrane made conformal contact with the resist. We used a UV light source (Karl Suss mask aligner, Model MJB3 UV400) to expose the resist for the experiments through the membrane. This aligner is equipped with a mercury lamp with emission peaks at 365, 405, and 436 nm; PDMS is largely transparent in this region (Fig. 7). The aligner provides a uniform, collimated illumination over an area >20 cm² with a variation of intensity <10%. After exposure, the PDMS membrane was removed from the exposed resist, and the resist was developed in a basic solution of sodium hydroxide (Shipley 351, diluted 1:5 in 18-MΩ water).
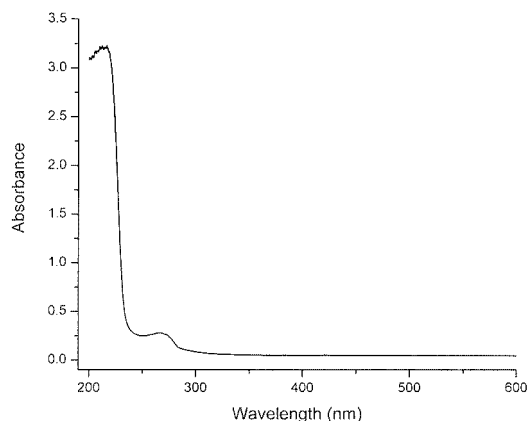
The surface topography of the photoresist was ex-amined with a SEM microscope (LEO 982 digital scanning electron microscope) operating at 1 keV.

3. Results and Discussion

A. Optical Elements without a Spacer on the Surface of Microlenses

1. Photolithography with High-Index Microspheres ($n_s > n_{PDMS}$)

Because n_{PS} (1.59) $> n_{PDMS}$ (1.4), PS spheres embedded in PDMS concentrate incident illumination on, and generate circular micropatterns in, photoresist. Figure 8(a) shows a ring-shaped pattern of photoresist generated by a single 3-μm PS sphere. With crystallized microspheres, multiple light scattering between spheres occurs; this effect can result in noncircular patterns. Figure 8(b) shows a hexagonal pattern of hexagonal holes on photoresist generated by a 2-D crystal of 3-μm spheres.

The importance of multiple scattering between spheres depends on several factors: (i) the distance between the spheres, (ii) the size of the spheres, and (iii) the composition of the spheres and the surrounding medium. If the distance between two spheres is larger than three times the diameter of the spheres, the effect of multiple scattering is usually sufficiently weak to be neglected.[19] For a 2-D crystal of spheres, multiple scattering of light plays an important role in generation of the pattern in the photoresist. Generally speaking, the smaller the spheres, the shorter the distances between them and thus the stronger the effect of multiple scattering.

Figure 8(c) shows arrays of circular holes produced by a 2-D crystal of 1-μm PS spheres. For spheres much larger than the incident wavelength, multiple scattering between spheres is weak, and the 2-D crystal of spheres generates arrays of circular holes. Figure 8(d) shows a pattern generated by a 2-D array of 10-μm PS spheres. The pattern consists of an array of circular holes with smaller triangular holes
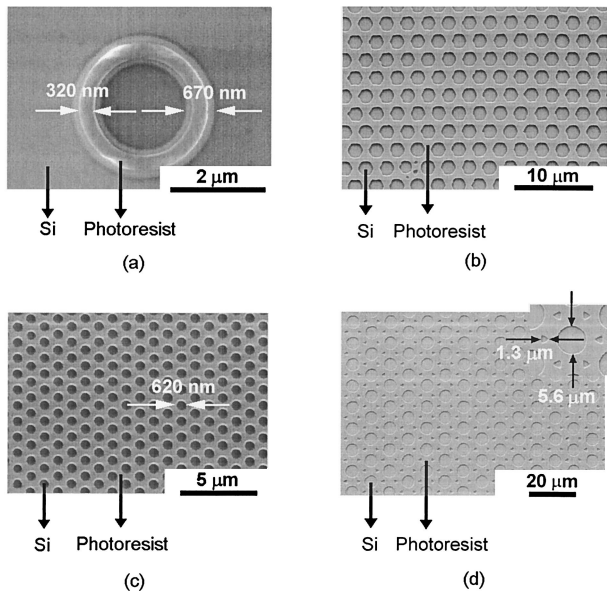
Fig. 8. SEM images of four representative patterns on photoresist generated by use of PDMS membranes with high-index spheres (PS spheres) embedded close to its surface ($t = 0$). (a) A ring-shaped micropattern generated by an individual 3-μm PS sphere, (b) a triangular array of hexagonal holes generated by a 2-D crystal of 3-μm spheres, (c) a triangular array of circular holes produced by a 2-D crystal of 1-μm PS spheres, (d) a pattern generated by a 2-D crystal of 10-μm PS spheres.

between three neighboring circular holes. Each triangular hole was produced by the gap between three neighboring spheres by the interference of incident light and light scattered from the three spheres.

2. Photolithography with Low-index Microspheres ($n_S < n_{PDMS}$)

Microspheres with an index smaller than that of the surrounding medium cause the incident illumination to diverge. The divergent light may enter neighboring spheres and contribute to multiple scattering: Low-index spheres cause stronger multiple scattering than do high-index spheres. We used two types of low-index sphere for our experiment: air spheres and silica spheres. The contrast of refractive indices between air spheres and PDMS (n_{air}:n_{PDMS} = 1:1.4) is higher than that between silica spheres and PDMS (n_{SiO_2}:n_{PDMS} = 1.37:1.4). Figure 9(a) shows a typical pattern generated by a single 1-μm air sphere. The width of the rings (220 nm) depends on resist thickness and exposure time. Figure 9(b) shows a pattern of an array of hexagons generated by a hexagonal array of 1-μm air spheres. Silica spheres do not concentrate light as well as PS spheres; they generate hexagonal or circular frames instead of deep holes in positive resist. Figure 9(c) shows a honeycomb pattern generated by a 2-D array of 1.4-μm silica spheres.

3. Lift-Off with Thin Films of Metals

Micropatterns produced by this technique can be transferred into metallic thin films by lift-off. Figure 10 shows patterns of thin films of metals formed by evaporation of Ti/Au onto patterned photoresist,
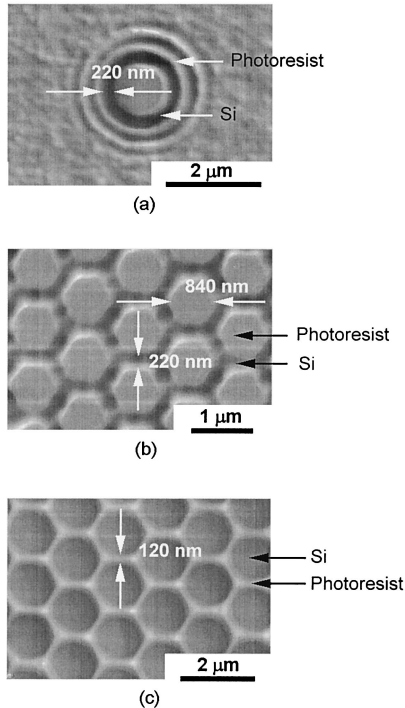

Fig. 9. SEM images of three representative patterns on photoresist generated by use of PDMS membranes with low-index spheres (air or silica spheres) embedded in the surface. (a) A pattern generated by an individual 1-μm air sphere, (b) a pattern generated by a triangular array of 1-μm air spheres, (c) a pattern generated by a 2-D hexagonal crystal of 1.4-μm silica spheres.
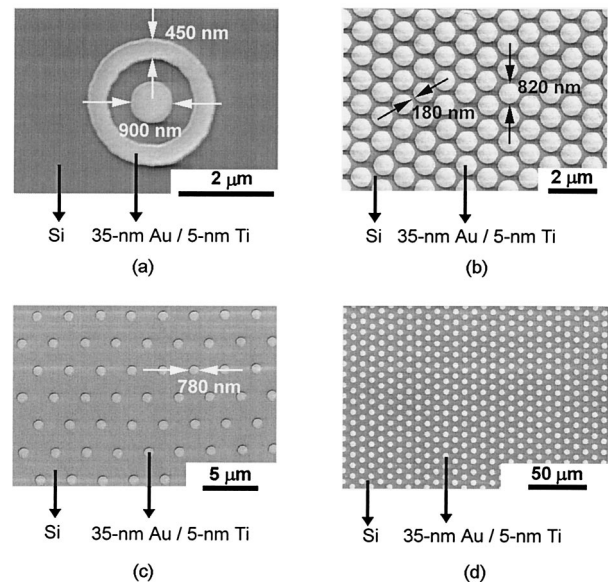

Fig. 10. SEM images of patterns of metal thin films (35-nm Au on 5-nm Ti) formed by lift-off of photoresist. The resist layer was patterned with PS spheres for photolithography ($t = 0$). (a) A pattern generated by a 1-μm PS sphere; (b) a pattern generated by a 2-D array of 1-μm PS spheres; (c) and (d) patterns produced with 3- and 10-μm PS spheres, respectively.
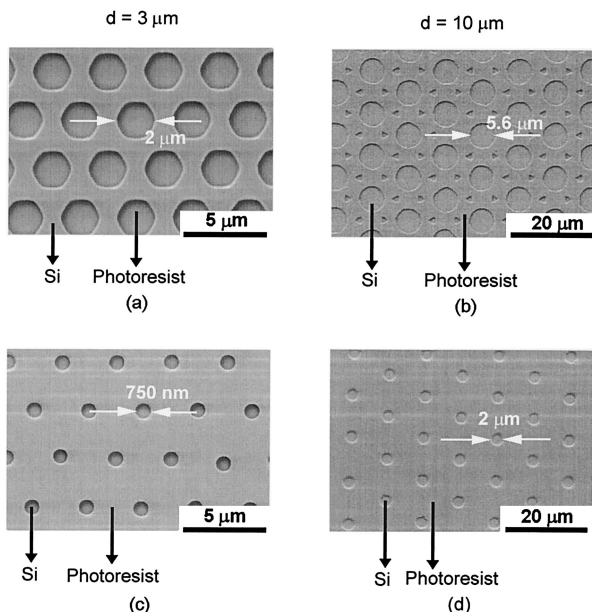
Fig. 11. SEM images showing a comparison between patterns of photoresist generated with PDMS membranes with and without a spacer between the embedded spheres and the surfaces of the membranes. (a) and (c) Arrays of micropatterns produced by embedded 2-D crystals of 3-μm spheres: (a) without a spacer and (c) with a 3-μm PDMS spacer. (b) and (d) Arrays of micropatterns produced by 2-D crystals of embedded 10-μm PS spheres embedded in PDMS: (b) without a spacer and (d) with a 10-μm PDMS spacer.

Fig. 12. SEM images of patterns on photoresist generated by use of wedge-shaped PDMS membranes ($\theta = 45°$) with a 2-D crystal of PS spheres embedded in the surface. (a) A horseshoe-shaped pattern generated by an individual embedded 3-μm PS sphere. (b) and (c) Arrays of micropatterns produced by embedded 2-D crystals of PS spheres by (b) 3-μm spheres and (c) 1-μm spheres.

followed by a lift-off of the photoresist in acetone. Figure 10(a) shows a pattern generated by a single 1-μm PS sphere. The patterns shown in Figs. 10(c) and 10(d) were produced with 3- and 10-μm PS spheres, respectively. Periodic patterns in metal thin films are useful in applications such as frequency-selective filtering.[1–3]

B. Pattern Generation by Exposure on Different Image Planes

An array of microlenses generates different optical patterns on different image planes. We can produce different optical patterns from the same array of microlenses by positioning the layer of photoresist at different distances from the array of microlenses. Figures 11(c) and 11(a) demonstrate the difference between patterns generated by arrays of 3-μm PS spheres with and without a 3-μm PDMS spacer. The membrane with the spacer generated arrays of smaller holes [Fig. 11(c)], because of the focusing of light by the microspheres. Figures 11(b) and 11(d) show similar results generated by 10-μm PS spheres, without and with a 10-μm-thick PDMS spacer.

C. Wedge-Shaped Membranes

Figure 4 indicates that the top surface of a wedge-shaped membrane refracts the incident illumination to an angle β. The embedded spheres project the deflected incident light obliquely onto the substrate. The oblique exposure on photoresist generates uni-
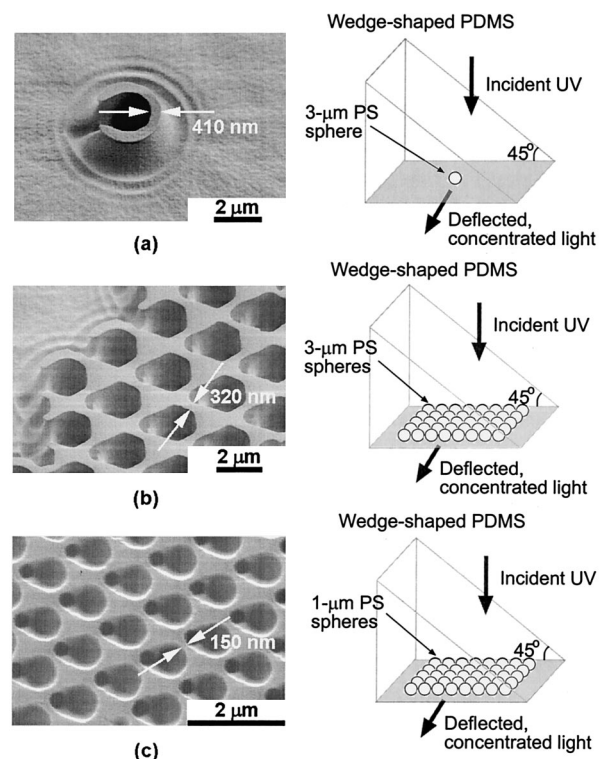
form arrays of distorted, noncircular features. Figure 12(a) shows a horseshoe-shaped pattern in photoresist generated by a 3-μm PS sphere embedded in a wedge-shaped membrane. Patterns shown in Figs. 12(b) and 12(c) were generated by wedge-shaped membranes with embedded arrays of 3- and 1-μm PS spheres, respectively. These patterns are uniform over a large area and may be useful in appropriate applications such as frequency-selective filtering.[40]

D. Tilted Membranes in Contact with Substrates

Figure 13 shows a flat PDMS membrane in contact with a resist layer and tilted at an angle θ; this geometry results in an oblique illumination of the microspheres and the photoresist. The deflected UV light is incident on the spheres at an angle $\gamma = \sin^{-1}(\sin \theta / n_{PDMS})$. Here, θ ranges from 0° to 90° and $n_{PDMS} \sim 1.4$; γ therefore varies from 0° to ~45°. This simple procedure allows deflection of UV light over angles between 0° and 45°. The microspheres cause the light to converge onto or diverge from the photoresist at an angle also equal to γ. The oblique exposure generates patterns in photoresist that do not have a symmetry axis (Fig. 13). Figure 13(a) shows a pattern produced by a single 1-μm PS sphere with the sample tilted at 50°. Figures 13(b) and 13(c) show patterns produced by a hexagonal array of

$$\gamma = \sin^{-1}(\sin\theta / n_{PDMS})$$
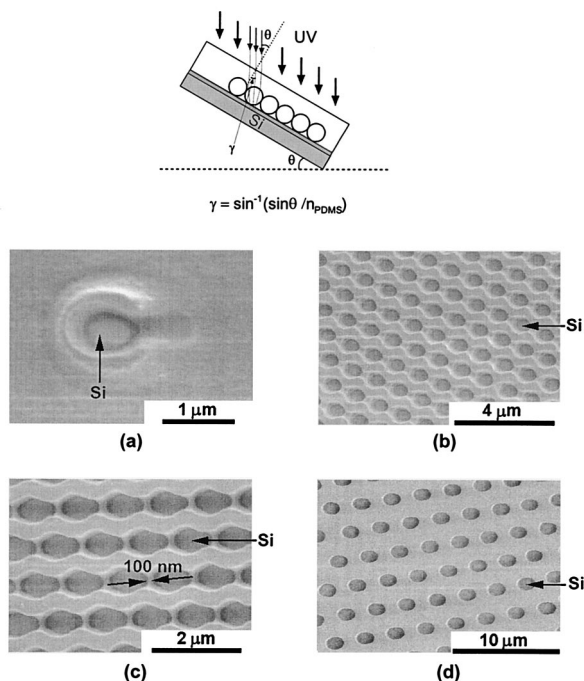

Fig. 13. SEM images of patterns on photoresist generated by oblique illumination. (a) A pattern generated by an individual 1-μm PS sphere embedded in a PDMS membrane tilted at 50°. (b) and (c) Patterns generated by a 2-D crystal of a 1-μm PS sphere embedded in a PDMS membrane tilted at different angles: (b) tilted at 50° and (c) tilted at 70°. (d) A pattern generated by an embedded 2-D crystal of 3-μm PS spheres with a 3-μm spacer; the PDMS membrane was tilted at 70°.

1-μm PS spheres with the substrates tilted at different angles during exposure. We generated the pattern shown in Fig. 13(b) by tilting the substrate at 50° for exposure, whereas the pattern in Fig. 13(c) was produced at 70°. The larger tilt angle in Fig. 13(c) resulted in narrower features (~100 nm) between neighboring holes. Figure 13(d) shows a pattern of an array of elliptical holes generated by a hexagonal array of 3-μm PS spheres with a 3-μm-thick spacer on the surface. We generated this pattern by tilting the substrate at 70° for exposure.

E. Photolithography by use of an Array of Plano–Convex Microlenses

A square array of circular plano–convex lenses focuses the incident illumination into the photoresist and generates a square array of circular holes with diameters smaller than the lenses. Similarly, a lenticular array can produce an array of parallel lines narrower than the width of the lenses on its focal plane.

The patterns produced by plano–convex lenses also depend on the image distance. We used two methods to adjust the image distance: (i) We fabricated a transparent spacer on top of the microlens array with the thickness of the spacer equal to the image distance, and (ii) we fabricated thin-film spacers on the edge of the lens array to generate a uniform air gap between the lens array and the resist layer. Figure
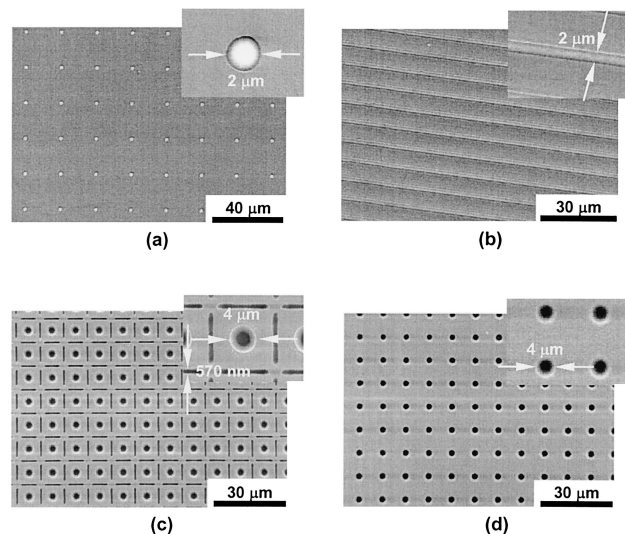

Fig. 14. SEM images of patterns generated by arrays of plano–convex microlenses. (a) A pattern generated by a square array of 10-μm plano–convex lenses [Fig. 6(c)] with a 13-μm air gap. The image distance is 10 μm. (b) An array of parallel trenches in photoresist produced by the 5 μm × 5 μm array of cylindrical microlenses [Fig. 6(d)] with a 5-μm air gap. (c) and (d) Patterns generated with the 5 μm × 5 μm grid lens shown in Fig. 2(a) with different spacers: (c) without a spacer and (d) with an 8-μm PDMS spacer coated on the grid lens.

14 shows the patterns generated by arrays of plano–convex microlenses. Figure 14(a) shows the pattern generated by a square array of 10-μm plano–convex lenses [Fig. 6(c)] with a 13-μm air gap. The pattern of parallel trenches in photoresist shown in Fig. 14(b) was generated with the 5 μm × 5 μm array of cylindrical lenses shown in Fig. 6(d) with a 5-μm air gap. Figures 14(c) and 14(d) show a comparison between the patterns generated with the 5 μm × 5 μm grid lens shown in Fig. 2(a) with different PDMS spacers. Figure 14(c) shows the pattern produced when we placed the grid lens on top of the photoresist without a spacer for exposure. The pattern shown in Fig. 14(d) was produced by an 8-μm PDMS spacer between the microlenses and the photoresist.

4. Conclusions

Use of 2-D arrays of microlenses can cause incident illumination to converge or diverge and can generate 2-D periodic optical patterns. We used 2-D arrays of microlenses for photolithography and demonstrated that the lens arrays can generate 2-D arrays of uniform micropatterns over areas of several square centimeters. In principle the size of the area that can be illuminated in parallel is limited only by the membrane and the uniformity of the flood illumination.

We used two types of microlens: transparent microspheres and fabricated plano–convex microlenses. Self-assembled 2-D arrays of microspheres act as dense-packed arrays of microlenses and generate hexagonal dense arrays of micropatterns. Because we used high-precision microspheres (variation in diameter <3%) for the experiment, the micropatterns

produced in photoresist are uniform. Although use of microspheres offers the advantage that it produces dense arrays of uniform micropatterns, there are also disadvantages. For example, there are often defects and grain boundaries in the 2-D crystals of spheres and thus in the corresponding micropatterns.[37] In our experiments, we made defect-free monolayers of microspheres with an area larger than 2 mm^2. It is technically difficult to produce defect-free monolayers with an area >1 cm^2. It is also difficult to produce a monolayer with uniform spacing between neighboring spheres over an area >1 mm^2.

Use of fabricated plano–convex microlenses can produce arrays of micropatterns with a variety of shapes and with a variety of arrangements other than hexagonal arrays. Although these lens arrays produce uniform micropatterns over areas >4 cm^2, it is not easy to use these lens arrays to generate dense patterns with submicrometer features. To produce such patterns requires use of dense arrays of microlenses with the size of each lens <10 μm. The fabrication of such arrays of lenses is technically routine although expensive.

The topography of the micropatterns produced by this technique also depends on the properties of the incident illumination, such as its polarization, coherence, and intensity distribution. For example, micropatterns generated by high-numerical-aperture lenses or microspheres are influenced by polarization.[41] Coherent illumination would result in interference of the scattered light produced by neighboring spheres. This interference would generate ripples in the areas between micropatterns. The broadband light source we used for exposure causes chromatic aberration in the micropatterns. The short optical path between the lens array and the photoresist reduces the separation of light components of different wavelengths and thus minimizes the blurring of the micropatterns produced in the photoresist. For simplicity, we restricted the investigation to the case of unpolarized, partially coherent illumination.

We believe that 2-D arrays of micropatterns produced by this technique will be useful for applications requiring simple and repetitive arrays, e.g., in frequency-selective surfaces,[1–3] flat-panel displays,[7,8] color filters, gratings, memory devices, sensor arrays,[42] and biochips. Conventional photolithography can be used to fabricate these arrays, but it is a relatively complicated technology, especially when large areas are required.[9] The technique we outline here is both simple and inexpensive and is potentially attractive where lateral resolution can be traded against cost.

References

1. D. M. Byrne, A. J. Brouns, F. C. Case, R. C. Tiberio, B. L. Whitehead, and E. D. Wolf, "Infrared mesh filters fabricated by electron-beam lithography," J. Vac. Sci. Technol. B **3,** 268–271 (1985).

2. E. A. Parker, S. M. A. Hamdy, and R. J. Langley, "Arrays of concentric rings as frequency selective surfaces," Electron. Lett. **17,** 880–881 (1981).

3. K. J. Kogler and R. G. Paster, "Infrared filters fabricated from submicron loop antenna arrays," Appl. Opt. **27,** 18–19 (1988).

4. J. D. Joannopoulos, R. D. Meade, and J. N. Winn, *Photonic Crystals* (Princeton University, Princeton, N.J., 1995).

5. C. Berger, N. Collings, R. Vökel, M. T. Gale, and T. Hessler, "A microlens-array-based optical neural network application," Pure Appl. Opt. **6,** 683–689 (1997).

6. J. Schwider, W. Stork, N. Streibl, and R. Vökel, "Possibilities and limitations of space-variant holographic optical elements for switching networks and general interconnections," Appl. Opt. **31,** 7403–7410 (1992).

7. R. Vökel, H. P. Herzig, P. Nussbaum, W. Singer, R. Dändliker, and W. B. Hugle, "Microlens lithography: a new approach for large display fabrication," Microelectron. Eng. **30,** 107–110 (1996).

8. M. Ida, B. Montmayeul, and R. Meyer, "New microlithography technique for large size field emission displays," in *Euro Display '96: International Display Research Conference* (American Society for International Science and Technology, Silver Spring, Md., 1996), pp. 177–180.

9. W. M. Moreau, *Semiconductor Lithography* (Plenum, New York, 1989), Chap. 8.

10. R. Dändliker, S. Gray, F. Clube, H. P. Herzig, and R. Vökel, "Non-conventional techniques for optical lithography," Microelectron. Eng. **27,** 205–211 (1995).

11. S. M. Sze, *VLSI Technology* (McGraw-Hill, Singapore, 1988), Chap. 4.3.

12. M. T. Gale, M. Rossi, J. Pedersen, and H. Schutz, "Fabrication of continuous-relief micro-optical elements by direct laser writing in photoresist," Opt. Eng. **33,** 3556–3566 (1994).

13. S. Hayashi, Y. Kumamoto, T. Suzuki, and T. Hirai, "Imaging by polystyrene latex particles," J. Colloid Interface Sci. **144,** 538–547 (1991).

14. M.-H. Wu and G. M. Whitesides, "Fabrication of arrays of two-dimensional micropatterns using microspheres as microlenses for projection photolithography," Appl. Phys. Lett. **78,** 2273–2275 (2001).

15. P. Nussbaum, R. Vökel, H. P. Herzig, M. Eisner, and S. Haselbeck, "Design, fabrication, and testing of microlens arrays for sensors and microsystems," Pure Appl. Opt. **6,** 617–636 (1997).

16. H. A. Biebuyck and G. M. Whitesides, "Self-organization of organic liquids on patterned self-assembled monolayers of alkanethiolates on gold," Langmuir **10,** 2790–2793 (1994).

17. Y. Lu, Y. Yin, and Y. Xia, "A self-assembly approach to the fabrication of patterned, two-dimensional arrays of microlenses of organic polymers," Adv. Mater. **13,** 34–37 (2001).

18. H. C. van de Hulst, *Light Scattering by Small Particles* (Dover, New York, 1981).

19. M. Kerker, *The Scattering of Light and Other Electromagnetic Radiation* (Academic, New York, 1969).

20. M. Born, and E. Wolf, *Principles of Optics*, 6th ed. (Pergamon, New York, 1980), Chap. 13.5.

21. C. F. Bohren and D. R. Huffman, *Absorption and Scattering of Light by Small Particles* (Wiley, New York, 1983).

22. M. Sasaki, T. Kurosawa, and K. Hane, "Micro-objective manipulated with optical tweezers," Appl. Phys. Lett. **70,** 785–787 (1997).

23. M. E. J. Friese, A. G. Truscott, H. Rubinsztein-Dunlop, and

N. R. Heckenberg, "Three-dimensional imaging with optical tweezers," Appl. Opt. **38,** 6597–6603 (1999).

24. J. P. Brody and S. R. Quake, "A self-assembled microlensing rotational probe," Appl. Phys. Lett. **74,** 144–146 (1999).

25. T. Yamasaki and T. Tsutusi, "Fabrication and optical properties of two-dimensional ordered arrays of silica microspheres," Jpn. J. Appl. Phys. **38,** 5916–5921 (1999).

26. R. D. Pradhan, J. A. Bloodgood, and G. H. Watson, "Photonic band structure of bcc colloidal crystals," Phys. Rev. B **55,** 9503–9507 (1997).

27. J. A. Rogers, K. E. Paul, and G. M. Whitesides, "Qualifying distortion in soft lithography," J. Vac. Sci. Technol. B **16,** 88–97 (1998).

28. J. Aizenberg, J. A. Rogers, K. E. Paul, and G. M. Whitesides, "Imaging profiles of light intensity in the near field: application to phase-shift photolithography," Appl. Opt. **37,** 2145–2152 (1998).

29. J. A. Rogers, O. J. A. Schueller, C. Marzolin, and G. M. Whitesides, "Wave-front engineering by use of transparent elastomeric optical elements," Appl. Opt. **36,** 5792–5795 (1997).

30. J. A. Rogers, K. E. Paul, R. J. Jackman, and G. M. Whitesides, "Using an elastomeric phase mask for sub-100 nm photolithography in the optical near field," Appl. Phys. Lett. **70,** 2658–2660 (1997).

31. Z. L. Liau, D. E. Mull, C. L. Dennis, R. C. Williamson, and R. G. Waarts, "Large-numerical-aperture microlens fabrication by one-step etching and mass-transport smoothing," Appl. Phys. Lett. **64,** 1484–1486 (1994).

32. A. Schilling, R. Merz, C. Ossmann, and H. P. Herzig, "Surface profiles of reflow microlenses under the influence of surface tension," Opt. Eng. **39,** 2171–2176 (2000).

33. C. B. Gorman, H. A. Biebuyck, and G. M. Whitesides, "Use of a patterned self-assembled monolayer to control the formation of a liquid resist pattern on a gold surface," Chem. Mater. **7,** 252–254 (1995).

34. E. Kim, G. M. Whitesides, L. K. Lee, S. P. Smith, and M. Prentiss, "Fabrication of arrays of channel waveguides by self-assembly using patterned organic monolayers as templates," Adv. Mater. **8,** 139–142 (1996).

35. A. Kumar and G. M. Whitesides, "Patterned condensation figures as optical diffraction gratings," Science **263,** 60–62 (1994).

36. Y. Xia, E. Kim, X.-M. Zhao, J. A. Rogers, M. Prentiss, and G. M. Whitesides, "Complex optical surfaces formed by replica molding against elastomeric masters," Science **273,** 347–349 (1996).

37. E. Kim, Y. Xia, X.-M. Zhao, and G. M. Whitesides, "Solvent-assisted microcontact molding: a convenient method for fabricating three-dimensional structures on surfaces of polymers," Adv. Mater. **9,** 651–654 (1997).

38. N. D. Denkov, O. D. Velev, P. A. Kralchevsky, I. B. Ivanov, H. Yoshimura, and K. Nagayama, "Mechanism of formation of two-dimensional crystals from latex particles on substrates," Langmuir **8,** 3183–3190 (1992).

39. J. L. Wilbur, R. J. Jackman, and G. M. Whitesides, "Elastomeric optics," Chem. Mater. **8,** 1380–1385 (1996).

40. T. K. Wu, *Frequency Selective Surface and Grid Array* (Wiley, New York, 1995).

41. V. Dhayalan, T. Standnes, J. Stamens, and H. Heler, "Scalar and electromagnetic diffraction point-spread functions for high-NA microlenses," Pure Appl. Opt. **6,** 603–615 (1997).

42. C. Van Berkel, B. P. McGarvey, and J. A. Clarke, "Microlens arrays for 2D large area image sensors," Pure Appl. Opt. **3,** 177–182 (1994).